Acta Biomaterialia 9 (2013) 6594–6605

Contents lists available at SciVerse ScienceDirect

Acta Biomaterialia

journal homepage: www.elsevier.com/locate/actabiomat

Ultrathin chitosan–poly(ethylene glycol) hydrogel films for corneal tissue engineering

Berkay Ozcelik [a], Karl D. Brown [b], Anton Blencowe [a], Mark Daniell [b], Geoff W. Stevens [a], Greg G. Qiao [a,*]

[a] Department of Chemical and Biomolecular Engineering, The University of Melbourne, Victoria 3010, Australia
[b] Centre for Eye Research Australia (CERA), Royal Victorian Eye and Ear Hospital, Peter Howson Wing, Victoria 3002, Australia

ARTICLE INFO

Article history:
Received 27 August 2012
Received in revised form 16 November 2012
Accepted 17 January 2013
Available online 29 January 2013

Keywords:
Corneal endothelium
Chitosan
Ultrathin film
Hydrogel
Tissue engineering

ABSTRACT

Due to the high demand for donor corneas and their low supply, autologous corneal endothelial cell (CEC) culture and transplantation for treatment of corneal endothelial dysfunction would be highly desirable. Many studies have shown the possibility of culturing CECs in vitro, but lack potential robust substrates for transplantation into the cornea. In this study, we investigate the properties of novel ultrathin chitosan–poly(ethylene glycol) (PEG) hydrogel films (CPHFs) for corneal tissue engineering applications. Cross-linking of chitosan films with diepoxy-PEG and cystamine was employed to prepare ~50 μm (hydrated) hydrogel films. Through variation of the PEG content (1.5–5.9 wt.%) it was possible to tailor the CPHFs to have tensile strains and ultimate stresses identical to or greater than those of human corneal tissue while retaining similar tensile moduli. Light transmission measurements in the visible spectrum (400–700 nm) revealed that the films were >95% optically transparent, above that of the human cornea (maximum ~90%), whilst in vitro degradation studies with lysozyme revealed that the CPHFs maintained the biodegradable characteristics of chitosan. Cell culture studies demonstrated the ability of the CPHFs to support the attachment and proliferation of sheep CECs. Ex vivo surgical trials on ovine eyes demonstrated that the CPHFs displayed excellent characteristics for physical manipulation and implantation purposes. The ultrathin CPHFs display desirable mechanical, optical and degradation properties whilst allowing attachment and proliferation of ovine CECs, and as such are attractive candidates for the regeneration and transplantation of CECs, as well as other corneal tissue engineering applications.

1. Introduction

Corneal endothelial cells (CECs) are specialized, polygonal-shaped cells that reside on the inner surface of the cornea within the aqueous chamber [1]. CECs are responsible for actively pumping fluids across the cornea to maintain corneal transparency [1]. Human CECs do not regenerate in vivo and upon loss of their function corneal transplantation is required to restore vision [1,2]. Various factors can lead to the loss of function of the CEC layer, including ageing, trauma and disease [1,3]. Once the number of these cells reduces below a critical value, the cornea loses its optical clarity due to oedema, which subsequently leads to blindness [1]. Various transplantation methods are available, ranging from the replacement of the whole cornea to the replacement of only the diseased cell layer [4–7]. As a result of the highly invasive nature of full-thickness corneal transplants, less invasive methods have been developed. For example, Descemet's stripping endothelial keratoplasty (DSEK) [8,9] involves removing the Descemet's membrane, along with the non-functioning CECs, from the cornea via a small incision into the anterior chamber. Subsequently, a thin layer of donor corneal endothelium supported by a section of the stroma is inserted into the anterior chamber to replace the CECs [8]. Since only a thin layer of tissue is replaced via a small incision, the technique is less invasive, healing rates are more rapid and the chances of infection are greatly reduced [9]. As with all types of corneal transplantation techniques utilizing donor tissue, there are also risks of rejection and graft failure with the DSEK procedure [9–11]. As such, development of an autologous transplant for the treatment of corneal endothelial dysfunction would be ideal.

A wide variety of substrates have been investigated for the regeneration and potential implantation of CECs [12–19]. In particular, collagen-based materials demonstrate desirable properties for the attachment and proliferation of CECs but generally have tensile strengths inferior to that of the human cornea [12–14]. The effects of harvesting, isolation and purification negatively impact upon the mechanical properties of collagen, whereby they are rapidly degraded due to disassembly of the natural structure and cross-links present in vivo [20]. Ultimately, this hinders their application in surgical procedures such as DSEK, which are physically demanding and require robust substrates for implantation. In addition, since most natural polymers are sourced from animals,

* Corresponding author.
E-mail address: gregghq@unimelb.edu.au (G.G. Qiao).

1742-7061/$ - see front matter © 2013 Acta Materialia Inc. Published by Elsevier Ltd. All rights reserved.
http://dx.doi.org/10.1016/j.actbio.2013.01.020

there are potential risks in regards to disease transmission [21,22]. Other materials, such as hyaluronic acid, amniotic membrane and silk fibroin, have also been investigated as potential substrates for CEC regeneration and transplantation with promising results [23–25]. These substrates have desirable tensile properties, support CEC attachment and proliferation, and were able to be implanted in vivo. However, there are certain issues associated with the use of such materials as implantable substrates. Hyaluronic acid requires modification for structural integrity and chemical stability [26] and silk fibroin has issues related to immune responses in vivo [27,28]. In addition, amniotic membrane, which is obtained from human donors in most cases, carries risks associated with disease transmission [29]. Furthermore, variation in the transparency of amniotic membranes depending on the source and location has been reported, which is a significant consideration for ophthalmic applications [30].

Rafat et al. recently demonstrated that cross-linking of collagen composites with a poly(ethylene glycol) (PEG)-dialdehyde derivative yielded thick hydrogel films (~500 μm) that displayed desirable properties for corneal tissue engineering [31]. Interestingly, the incorporation of small amounts of chitosan (1 wt.% relative to collagen) into the composites led to significant improvements in the strength and elasticity of the hydrogels. The hydrogels were subsequently used to replace the majority of the cornea in animal subjects via deep lamellar keratoplasty and displayed good biocompatibility over a period of 120 days. Liang et al. also demonstrated that chitosan, gelatin and chondroitin sulfate composite membranes are capable of supporting the regeneration of rabbit CECs, thus highlighting the suitability of chitosan-based materials for corneal engineering applications [20].

Chitosan is a linear polysaccharide consisting of randomly distributed glucosamine and *N*-acetylglucosamine repeat units and is derived from *N*-deacetylation of chitin, the world's second most abundant polysaccharide after cellulose [32]. Chitosan's biocompatible, biodegradable and non-toxic nature has resulted in significant interest in its use within the biomedical field [33,34]. In addition, its antimicrobial and antifungal properties, and low immunogenicity make chitosan an attractive polymer for medical applications [35,36], particularly wound healing [37,38]. Furthermore, chitosan has also been extensively investigated as a material for various tissue engineering applications. As a result of chitosan's many amine and hydroxyl functional groups, it can be readily cross-linked and modified to afford hydrogels suitable for drug delivery, cartilage and skin regeneration and adipose tissue engineering [39–43].

PEG is a water-soluble, hydrophilic polymer that has been widely explored for biomedical applications due to its non-toxic, minimal immunogenicity and anti-protein fouling properties [44–47]. As the US Food and Drug Administration (FDA) has approved this polymer for use in drug and cosmetic applications [44], PEG has also been investigated to prepare hydrogel scaffolds for tissue engineering applications [48]. Many in vitro and in vivo studies have demonstrated the desirable properties of PEG, as well as the cell and tissue penetration and vascularization capability of scaffolds fabricated using PEG [49–52].

Several studies have investigated the combination of chitosan and PEG to prepare potential tissue engineering scaffolds [53–55]. As such, combining the advantageous properties of both PEG and chitosan, we herein report the fabrication of ultrathin, biocompatible and biodegradable chitosan–PEG hydrogel films (CPHFs) for the regeneration and implantation of CECs. The CPHFs are prepared via the cross-linking of chitosan films with diepoxy-PEG and cystamine. The judicious introduction of disulphide-containing cystamine during the PEG cross-linking step imparts additional points of degradation within the films as well as branching for the cross-linking. The resultant optically transparent and permeable films have excellent mechanical properties that surpass the tensile strength of the human cornea whilst retaining similar elastic moduli, and, as such, are well suited to ophthalmic applications. Their mechanical properties combined with a thicknesses of just 50 μm make these films particularly desirable for minimally invasive implantation procedures resembling DSEK. In vitro studies revealed that the CPHFs supported the proliferation of CECs from sheep sources, thus demonstrating their potential for corneal tissue engineering.

2. Experimental

2.1. Materials

Chitosan from fresh shrimp shells (*Pandalus borealis*) (190–310 kDa; ~80% deacetylated), cystamine dihydrochloride (98%), poly(ethylene glycol) diglycidyl ether (PEGDGE) (M_n = 526 Da), collagen Type I from calf skin (0.1% solution, sterile filtered), phosphate-buffered saline (PBS) tablets, glucose assay kit (Sigma GAGO-20: glucose oxidase/peroxidise reagent and *O*-dianisidine dihydrochloride) and albumin–fluorescein isothiocyanate conjugate from bovine (albumin-FITC), insulin, transferrin, selenium, 4′,6-diamidino-2-phenylindole (DAPI) fluorescent stain, Triton X-100, and dextran $M_r \approx 500000$ were obtained from Sigma–Aldrich. Dulbecco's Modified Eagle's Medium:Nutrient Mixture F12 (DMEM:F12), antibiotic–antimycotic, epidermal growth factor (EGF), fetal calf serum (FCS), Alexa Fluor 488 goat anti mouse IgG, trypsin, and EDTA were obtained from Invitrogen. Anti-Na^+/K^+-ATPase (β2-subunit) monoclonal IgG produced in mouse clone M17-P5-F11 was obtained from Santa Cruz Biotechnology. Thermanox tissue culture plastic (TCP) coverslips were obtained from NUNC. D-Glucose (anhydrous) was obtained from Chem-Supply. Cystamine dihydrochloride was neutralized according to a previously published procedure [52]. Tetrahydrofuran (THF) (Honeywell, 99.99%), sodium hydroxide (Merck, >99%), acetic acid (Chem-Supply, >99.7%) were used as received. Milli Q water (18.2 MΩ cm) was obtained from a Millipore Synergy Water system. Poly(vinyl chloride) (PVC) sheets were obtained from Bunnings Warehouse, Australia. Deuterium oxide (99.8% D) was purchased from Cambridge Isotope Laboratories and used as received. Matrix-assisted laser desorption/ionization time-of-flight mass spectroscopy (MALDI ToF MS) matrices (α-cyano-4-hydroxycinnamic acid (α-CHCA) (⩾99.5%), *trans*-2-[3-(4-tert-butylphenyl)-2-methyl-2-propenylidene]malononitrile (DCTB) (⩾99.0%), 2,5-dihydroxy benzoic acid (DHB)), and cationization agent (NaTFA (99.999%)) were purchased from Aldrich and used as received.

2.2. Instrumentation

Thermogravimetric analysis (TGA) was conducted using a Perkin-Elmer Diamond TGA/DTA with Pyris Thermal Analysis Software. Environmental scanning electron microscopy (E-SEM) was carried out using a FEI Quanta FEG 200 Enviro-SEM with the samples mounted on carbon tabs. UV–Vis light transmittance measurements were carried out using a Shimadzu UV-1800 UV–Vis scanning spectrophotometer. A side-by-side diffusion cell with magnetic stirrers was obtained from PermeGear Inc. Mechanical testing was conducted using an Instron Microtester 5848 equipped with Bluehill material testing software. Spectral reflectance measurements were obtained using a Filmetrics thin-film measurement system with the F20-XT configuration. Immunofluorescence imaging was carried out using a Olympus BX61 system with computer-assisted stereographic tomography (CAST) (Olympus, Japan). ^{1}H nuclear magnetic resonance (NMR) spectroscopy was performed using a Varian Unity400 spectrometer operating at 400 MHz (using the deuterated

solvent as lock). MALDI ToF MS was performed on a Bruker Autoflex III mass spectrometer operating in positive/linear mode. The matrix (DHB, DCTB or α-CHCA) and cationization agent (NaTFA) were dissolved in methanol (10 and 1 mg ml^{-1}, respectively) and then mixed with the analyte in a ratio of 10:1:1. 0.3 μl of this solution was then spotted onto a ground steel target plate and the solvent allowed to evaporate prior to analysis. FlexAnalysis (Bruker) was used to analyze the data. The values quoted correspond to the molecular weight of the species.

2.3. Preparation of CPHFs

2.3.1. Casting of chitosan films

Chitosan (1 g) was suspended in Milli Q water (99 ml) with stirring and acetic acid (1 ml) was added. The clear, viscous solution was stirred for 15 min and then centrifuged at 4400 rpm for 5 min. The centrifuged solution was pipetted onto a smooth PVC sheet so that 0.21 ml of 1% chitosan solution was pipetted for every cm^2 of the PVC surface. A spirit level was used prior to pipetting of the chitosan solution, to ensure that the containers were flat and an even coverage with the solution was obtained. The solution on the coated PVC sheet was then degassed for 1 h under vacuum (0.1 mbar) prior to being placed in an oven at 30 °C with an opening to allow for water evaporation for 24 h. The resulting chitosan film was peeled off the PVC sheet, immersed in 1 M NaOH (20 ml) for 10 min and then washed with Milli Q water (3 × 200 ml). Subsequently the films were dried in vacuo (20 mbar) at 60 °C for 2 h and stored in a glass container until further use.

2.3.2. Cross-linking of chitosan films

PEGDGE was dissolved in THF with agitation to afford 10, 30, 50 and 70% v/v solutions or used neat. Cystamine was added in a 4:1 PEGDGE:cystamine molar ratio and the solution was mixed thoroughly. Dry chitosan films were placed into solutions both with and without cystamine at a volume to mass ratio of 65 ml solution/g chitosan film. After 24 h at 25 °C the resulting CPHFs were removed and soaked in THF (50 ml, 3 × 15 min) before being washed thoroughly with Milli Q water (3 × 200 ml). The CPHFs were then dried in vacuo (20 mbar) at 60 °C for 24 h and stored in a glass jar until further use. No additional surface modification or extracellular matrix (ECM) coating was carried out on the CPHFs following PEGDGE and cystamine cross-linking. To observe the swelling characteristics, CPHFs were placed in 1 × PBS for 24 h. The percentage equilibrium swelling ratio (%ESR) of the films was calculated using the equation $\%ESR = [(W_s - W_d)/W_d] \times 100\%$, where W_s and W_d refer to the swollen and dried weights, respectively. The analysis was conducted in triplicate for each type of CPHF and the results averaged.

2.4. Thickness analysis of CPHFs

E-SEM and spectral reflectance analysis was used to determine the thickness of the CPHFs. Dried CPHFs mounted on carbon tabs were analyzed via E-SEM under low-vacuum conditions. The tilt adjustment of the sample holder was used to observe the cross-section of the CPHFs. Subsequently, ImageJ software (National Institute of Health, USA) was used to determine the average thickness. Spectral reflectance measurements of the dried and hydrated CPHFs were conducted in air with a film refractive index of 1.459, at different locations on the films. Thickness values were obtained from an average of three measurements between wavelengths of 1600 and 1650 nm using the Filmetrics F20-XT configuration.

2.5. Light transmittance evaluation of CPHFs

Dried CPHFs were swollen in 1 × PBS solution prior to UV–Vis evaluation. Light transmittance measurements were recorded at 25 °C over the visible spectrum (350–750 nm).

2.6. In vitro degradation of CPHFs

Dried CPHFs prepared from cross-linking with 50% v/v PEGDGE/cystamine solutions ($CPHF_{50}$) were cut into 2 cm × 2 cm squares. Lysozyme (4.8 g) and L-cysteine (0.825 g) were dissolved in PBS (750 ml) to afford a solution containing a 100 times greater concentration of lysozyme and L-cysteine than that found in the human aqueous humour [56,57]. The solution was separated into 15 glass containers (50 ml) and the CPHF squares were weighed and then placed into each of the solutions. The containers were sealed and placed in a temperature-controlled orbital shaker at 35 °C. Three containers were removed from the orbital shaker at time points of 3 days, and 1, 2, 4 and 8 weeks. The remaining films were carefully removed from the containers, immersed in Milli Q water (25 ml) for 15 min with occasional gentle agitation, dried in vacuo (20 mbar) at 60 °C for 24 h under vacuum and then weighed. The mass remaining was plotted against time to obtain the degradation profile of the films.

2.7. Compositional characterization of CPHFs

For TGA, CPHFs (2 cm × 2 cm) were dried in vacuo (20 mbar) at 60 °C for 24 h prior to analysis. The dried CPHFs, unmodified chitosan film and PEGDGE were individually subjected to TGA to determine their degradation profiles. Each sample was loaded into a porcelain crucible and after 30 min was weighed. The samples were heated to 500 °C at a rate of 5 °C min^{-1}. The thermal degradation data obtained by the TGA was analyzed using OriginPro 7.5 software. For NMR spectroscopic analysis and MALDI ToF MS the dried CPHFs (0.3 g) were placed in fuming hydrochloric acid (37% HCl) (20 ml) and stirred at 70 °C for 22 h. The HCl was removed in vacuo and the residue was azeotroped with Milli Q water (5 × 50 ml). The resultant powder was suspended in methanol (5 ml) and centrifuged. The supernatant was then analyzed via MALDI ToF MS. The methanol supernatant was then dried in vacuo and the residue was suspended in isopropanol (2 ml) and sonicated for 30 min. The suspension was then centrifuged and the supernatant was removed and dried in vacuo. The resultant light yellow powder was then dissolved in D_2O (1 ml) and analyzed via ^1H NMR spectroscopy.

2.8. Evaluation of tensile properties of CPHFs

CPHFs were swollen in 1 × PBS and then cut into 4 cm × 2 cm pieces for evaluation of their tensile properties. The films were clamped between wooden tabs within the metal clamps of an Instron Microtester 5848 to prevent slippage and jaw tearing of the films (gauge area 2 cm × 2 cm). CPHFs were not stress preconditioned prior to tensile testing. Tensile evaluation of the CPHFs was carried out in the water bath of the microtester in 1 × PBS solution at 35 °C. At least three repeats from each cross-linking condition were used in the tensile evaluation. Samples were stretched at a rate of 0.1 mm s^{-1} until breakage of the films in the gauge area occurred. Any film that did not break within the gauge area was disregarded for compilation of raw data. To determine the effects of in vitro conditions on the tensile properties, the CPHFs (4 cm × 2 cm) were maintained in DMEM (supplemented with 10% v/v FBS, 1% v/v penicillin–streptomycin, 1% v/v L-glutamine) for 14 days (37 °C, 5% CO_2) and subsequently subjected to the same tensile evaluation. Data obtained from the Bluehill

software was analyzed using OriginPro 7.5 software to determine the ultimate tensile stress–strain and tensile modulus.

2.9. In vitro cytotoxicity assessment of CPHF degradation products

Dried CPHFs (5 g) were placed in fuming hydrochloric acid (37% HCl) (30 ml) and stirred at 70 °C for 18 h. The HCl was removed in vacuo and the residue was azeotroped with Milli Q water (5 × 100 ml) until a neutral pH was obtained. The resulting light brown powder was stored in a desiccator until further use. For the cytotoxicity study 3T3 fibroblasts were passaged and seeded onto 2 × 6 well plates at 75,000 cells per well. The degradation products were dissolved in sterile DMEM to provide a 4 mg ml^{-1} stock solution. 10 and 1000 μl of the stock solution was added to the wells and the total volume in the wells was made up to 4 ml to obtain degradation product concentrations of 10 and 1000 ppm, respectively. The wells were then placed in a 37 °C, 5% CO_2 incubator for 72 h. Following incubation, the morphology of the cells was observed under a microscope. Cells in each well were trypsinized and the numbers of viable cells were counted using a haemocytometer following staining with trypan blue.

2.10. In vitro permeability evaluation of CPHFs

Glucose and albumin diffusivity measurements were carried out using a side-by-side diffusion cell (PermeGear, Bethlehem, PA) with cell volumes of 5 ml. The CPHF was placed between the two cells and clamped tightly. For glucose measurements, the source cell was filled with glucose in PBS (0.05 g ml^{-1}, 4 ml) and the receiving cell with PBS buffer only (4 ml). For albumin measurements, 50 μM albumin-FITC in PBS (4 ml) was placed in the source cell and PBS (4 ml) in the receiving cell. For both glucose and albumin measurements the chambers were maintained at 35 °C with magnetic stirring in each cell. At set times (30, 45, 60, 80 and 100 min) 2 ml aliquots were removed from the receiving cell and replaced with fresh PBS (2 ml). For glucose measurements, the aliquots were prepared for spectrophotometric analysis using a glucose assay kit (Sigma GAGO-20: glucose oxidase/peroxidise reagent and *O*-dianisidine dihydrochloride reagent) and analysed using a Shimadzu UV-1800 spectrophotometer at 540 nm. For albumin measurements, the absorbance of the albumin-FITC at 495 nm was measured using a Shimadzu UV-1800 spectrophotometer.

2.11. Evaluation of attachment and proliferation of sheep CECs on CPHFs

2.11.1. Preparation of CPHFs for cell culture studies

CPHFs were hydrated in 1 × PBS (50 ml) and cut into circular disks (diameter 16 mm) using a circular hole punch. No surface modification or ECM coating was carried out on the CPHFs prior to the in vitro studies. Subsequently, the films were immersed in 80% v/v ethanol for 1 h. The films were then immersed in sterile PBS solution for 15 min (3 × 50 mL) and placed into a 24 well plate with sterile glass rings (external diameter 15 mm) to hold them in place. PBS (2 ml) was added to the wells and the plate was stored at 8 °C prior to cell culture studies.

2.11.2. CEC harvesting and in vitro cell seeding of CPHFs

Eye orbs from fresh scavenged experimental cadavers of merino sheep were washed with proviodine (1:50, 8 min), methanol (20% v/v, 60 s), peracetic acid (0.1% v/v, 5 min), and in PBS with antibiotic–antimycotic. Corneas were then dissected and transferred to thinning media (1:1 DMEM:F12, insulin (0.5 μg ml^{-1}), transferrin (0.275 μg ml^{-1}), selenium (0.25 ng ml^{-1}), EGF, 2% FCS, antibiotic–antimycotic and dextran) for 16 h. Descemet's membrane was dissected from corneal tissues, and treated with collagenase (2 mg ml^{-1}) for 60 min followed by trypsin (0.05%)–EDTA (0.02%) for 5 min. Descemet's membrane in the samples was then cut into small pieces and triturated to produce a single-cell suspension, subsequently the decellularized Descemet's fragments were removed. 25000 and 50000 cells were seeded onto CPHFs or Thermanox TCP coverslips in corneal media (1:1 DMEM:F12, insulin 0.5 μg ml^{-1}, transferrin 0.275 μg ml^{-1}, selenium 0.25 ng ml^{-1}, EGF, 10% FCS and antibiotic–antimycotic). Cell culture was performed under standard conditions (37 °C, 5% CO_2) for 7 days.

2.11.3. Immunofluorescence

Descemet's membranes dissected from sheep corneas were used as positive controls. Test samples were cultured sheep CECs on various test surfaces, CPHF and TCP. Negative control samples were not incubated with the primary antibody. All samples were fixed with 4% paraformaldehyde for 10 min before washing in PBS, and stored at 4 °C until use. Immunofluorescence was performed as follows. Samples were permeabilized with 0.3% Triton X-100 for 15 min before washing with PBS. Blocking was with 3% normal goat serum for 30 min. Samples were incubated with the primary antibody in PBS for 2 h in a humidified chamber. The negative controls were incubated without a primary antibody (Anti-Na^+/K^+-ATPase IgG antibody). After PBS washing the samples were incubated with the secondary antibody for 1 h (Alexa Fluor 488). After PBS washing samples were incubated with DAPI for 5 min. After a final PBS wash, samples were mounted with aqueous medium. Images were obtained using an Olympus BX61. CAST (Olympus) was used to determine cell density from DAPI-labelled nuclei. For comparison, the cell density of freshly dissected ovine corneas was determined by confocal microscopy and CAST.

2.12. Ex vivo surgical evaluation of CPHFs using ovine eyes

Whole sheep eyes were extracted from sacrificed sheep and mounted on polystyrene foam using a surgical needle for ex vivo evaluation. CPHFs prepared from the 50% v/v PEGDGE solution ($CPHF_{50}$), were cut into 9 mm diameter disks for surgical assessment. Two small incisions were initially made on opposite sides of the ovine cornea using a slit knife. The CPHF disks were placed on top of the cornea and were subsequently pulled into the anterior chamber using fine vitreo-retinal forceps. Saline solution was used to keep the sheep orb hydrated throughout the procedure. Following the insertion of the CPHF into the anterior chamber, air bubbles were introduced to allow the film to flatten and adhere onto the inner surface of the cornea. Photographs were obtained and the robustness of the film for use in the DSEK procedure was qualitatively assessed.

3. Results and discussion

3.1. Fabrication of CPHFs

As a result of their versatile properties, availability, processability and potential in biomedical research, chitosan and PEG were chosen as the main constituents for the fabrication of ultrathin hydrogel films (CPHFs). The precursor chitosan films were initially cast onto PVC sheets from dilute acetic acid solutions at 30 °C for 24 h (Fig. 1a). Casting of chitosan films on glass surfaces, i.e. glass Petri dishes, resulted in strongly adhered films that were difficult to remove without damaging the film. Hence PVC sheets were preferred for the chitosan film-casting process, since the chitosan films could be removed easily from these surfaces. Casting temperatures above 30 °C without degassing led to imperfections in the films as a result of bubble formation, which is non-desirable for optical applications where a smooth, defect-free surface is required

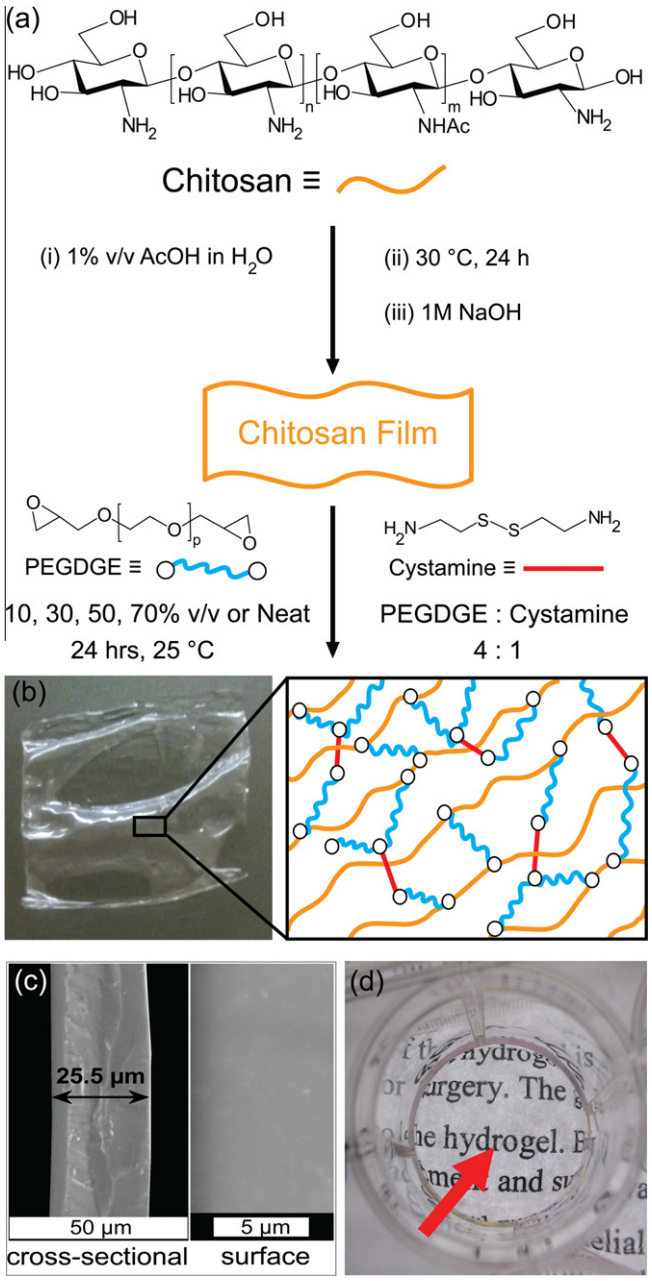

Fig. 1. (a) Synthesis of CPHF films. (b) Swollen CPHF with schematic showing cross-linked structure. (c) SEM images of the dehydrated CPHF cross-section and surface (note the smoothness and lack of defects). (d) $CPHF_{50}$ folded in half in PBS solution. Transparency of the film makes observation with the naked eye difficult. The arrow is pointing at the location of the fold in the film to demonstrate transparency even when film thickness is doubled.

to prevent refraction of incoming light and distortion of images. The films were subsequently treated with 1 M NaOH solution, washed with water and dried to afford stiff chitosan films that readily absorbed water, leading to elastic films that were robust enough to handle repeated stretching. NaOH treatment was carried out to neutralize any residual acetic acid and the protonated chitosan amino groups, thus making the chitosan film insoluble in water.

The neutralized and dried chitosan films were subsequently cross-linked using epoxy–amine chemistry through reaction of the amino groups present on the glucosamine repeat units with a diepoxy-PEG, PEGDGE and cystamine in solution (Fig. 1a). Epoxy–amine reactions are simple, stepwise reactions that have been widely studied for various applications [58–61], including the fabrication of hydrogel scaffolds for tissue engineering [52]. Solutions of PEGDGE in tetrahydrofuran (10, 30, 50 and 70% v/v, and neat) containing cystamine at a 4:1 PEGDGE:cystamine molar ratio were used to afford the CPHFs (referred to as $CPHF_X$, where x corresponds to the concentration of PEGDGE in the cross-linking solution, e.g. $CPHF_{30}$) (Fig. 1b). The chitosan films were immediately placed into the PEGDGE solutions with and without cystamine: the epoxy groups of the PEGDGE then react with the chitosan amino groups, resulting in cross-linking of the chitosan chains. Cystamine was selected to aid the cross-linking as it can react with the epoxy groups of PEGDGE to form branched cross-linking structures, and to introduce disulfide groups into the network, which provides additional degradation points that can be cleaved by cysteine and glutathione in vivo. A 4:1 PEGDGE:cystamine molar ratio was selected to maximize the formation of branch points without the formation of a cross-linked gel network from PEGDGE and cystamine. Thus, cystamine aids in the cross-linking of the chitosan film by generating multifunctional cross-linkers through reaction with PEGDGE. Tetrahydrofuran was used as the solvent due to the insolubility of chitosan in organic solvents [62]; hence, the chitosan film could be cross-linked without dissolution. Visual examination of the films following cross-linking revealed no observable differences between the initial chitosan film and the PEGDGE cross-linked films (CPHFs); however, upon addition of CPHFs treated with added cystamine to aqueous acetic acid (5% v/v), they remained intact and retained optical clarity, whilst the initial chitosan film readily dissolved. In comparison the chitosan films that were treated with PEGDGE without cystamine also readily dissolved similar to the untreated chitosan films, indicating that without cystamine incorporation, cross-linking of the chitosan film did not occur. This could be the result of branched cross-linkers formed due to the reaction between PEGDGE and cystamine that are able to increase the probability of cross-linking and allow the incorporation of PEG. Since multi-epoxy functional cross-linkers can be formed through the reaction between cystamine and up to four PEGDGEs, this would provide more potential cross-linking points, improving the chances of cross-linking with chitosan.

3.2. Thickness analysis

The thickness of the CPHFs was analyzed via E-SEM and spectral reflectance analysis. Cross-sectional and surface analysis of the dried CPHFs via E-SEM provided a dehydrated thickness of ~26 μm and displayed the smooth and imperfection-free topology of the films (Fig. 1c). The film thicknesses were also confirmed by spectral reflectance measurements that provided dehydrated and hydrated thicknesses of ~25 and ~46 μm, respectively. DSEK and similar lamellar keratoplasties such as Descemet's membrane endothelial keratoplasty (DMEK) utilize 10–150 μm thick grafts [63,64], and thus the thickness of the CPHFs is well suited for such applications. Previous studies using much thicker gelatin and hyaluronic acid films (650–800 μm) for corneal endothelial tissue engineering [65,66] require much more invasive procedures such as penetrating keratoplasty for implantation compared to the 50 μm CPHFs, which could be easily inserted via small incisions in the cornea. Whereas the thickness of the films for the purpose of these studies was chosen to be ~50 μm, alteration of the initial chitosan concentration and/or the amount of solution used for casting allows the thickness of the films to be tailored for specific applications.

3.3. Light transmittance evaluation

The human cornea allows transmittance of light in a monotonically increasing manner, whereby UV-light transmittance increases

from approximately 30% to 75% (310–400 nm) and the transmittance of visible light continues to increase from ~75 to 95% (400–700 nm) [67–69]. Any films for corneal applications should be at least as capable as the human cornea with respect to the transmittance of visible light in order not to hinder the vision of the host. As a result of their high transparency and 50 μm thickness, the CPHFs are almost invisible to the naked eye in water (Fig. 1d). UV–Vis spectroscopic analysis of all the CPHFs revealed that they transmit >95% of visible light at all wavelengths (400–700 nm) (Fig. 2), whereas the UV light transmittance reduces from 400 to 220 nm (Fig. 2). The transmittance of the CPHFs to UV and visible light is therefore similar to the human cornea. The potential effect of the implanted CPHFs on corneal transmittance would be minimal as DSEK-like procedures only remove a very thin layer of the cornea and replace it with a thin layer, leaving the majority of the cornea intact. In addition, the CPHFs are designed to biodegrade, and therefore any effect that they have on the light transmittance of the cornea would ultimately be eliminated. To prevent hindrance of the patient's vision, it is desired that the CPHFs are at least as capable as the human cornea in terms of the transmittance of visible light. The transmittance profile (Fig. 2) of the CPHFs reveals that they are easily capable of achieving this objective throughout the visible spectrum.

3.4. Compositional characterization of CPHFs

To determine the composition of the CPHFs, TGA was carried out to study the thermal degradation characteristics of the chitosan and PEG components. Initially, the unmodified chitosan film and the PEGDGE precursor were analyzed and the results were plotted as first-derivative thermogravimetric curves, which revealed degradation peaks at 280 and 340 °C, respectively (Fig. 3a and b). In comparison, TGA of the CPHFs revealed a peak corresponding to the chitosan at ~280 °C with a shoulder at ~340 °C corresponding to the PEG component (Fig. 3c), thus indicating the successful incorporation of PEG. Interestingly, the intensity of the shoulder increased as the concentration of PEGDGE used to cross-link the chitosan film increased up to 50%, with further increases in concentration resulting in a decrease in the intensity of the shoulder (Fig. 3c). In comparison the chitosan films treated without cystamine demonstrated identical TGA profiles to that of the unmodified chitosan film (Fig. 3c). The shoulders that indicate the incorporation of PEG into the CPHFs were not present in the TGA, hence indicating that PEG incorporation into the films did not occur in films treated without cystamine. This could be due to the multifunctional epoxy cross-linkers that form between cystamine and up to four PEGDGEs, increasing the cross-linking potential due to the additional cross-linking points formed.

The wt.% of PEG in the CPHFs was determined via analysis of the degradation rates of CPHFs and comparison to that of chitosan and PEGDGE. These were plotted against the concentration of PEGDGE in the cross-linking solutions (Fig. 3d), which revealed an increase followed by a decrease in wt.% with increasing PEGDGE concentration, demonstrating a "Gaussian-like" trend. This increase and subsequent reduction in PEG content could result from an increase in viscosity of the cross-linking solution when the concentration of PEGDGE is increased. The increased viscosity may limit reaction between the PEGDGE and the chitosan amino groups as higher viscosities reduce the mobility of the PEG chains and hinder their penetration into the chitosan film. The CPHFs demonstrated similar swelling characteristics to that of the control chitosan film. Regardless of the PEGDGE concentration used for the swelling, negligible differences were observed in regards to the %ESR between the different films (Table 1). Since chitosan is the major component in all CPHFs and is capable of swelling, the effect of small amounts of PEG incorporated into the CPHFs is negligble, and hence the difference between the films prepared with varying PEGDGE concentrations and the chitosan film is negligible.

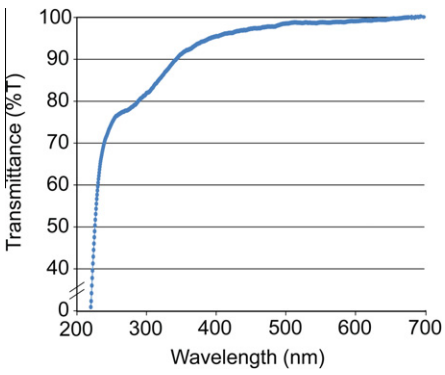

Fig. 2. Light transmission of CPHF across the UV–visible spectrum.

For ^{1}H NMR spectroscopic analysis and MALDI ToF MS initially the CPHFs were acid hydrolyzed in concentrated HCl via a similar method to that previously described [70,71]. ^{1}H NMR spectroscopic analysis and MALDI ToF MS of the HCl-mediated degradation products of the CPHFs confirmed the incorporation of PEG into the cross-linked chitosan films (Fig. 4). ^{1}H NMR spectroscopic analysis revealed characteristic resonances corresponding to the anomeric proton of the glucosamine repeat units at δ_H 5.40 ppm, as well as the methine protons of the glucosamine ring between δ_H 3.20 and 4.00 ppm (Fig. 4a). Incorporation of cystamine into the CPHF network was also evident with resonances observed for methylene protons adjacent to the disulfide and amino groups at δ_H 2.60 and 2.90 ppm, respectively. Amongst the resonances observed for glucosamine, methylene protons of the PEG chains were also observed at δ_H 3.70 ppm, indicating the incorporation of PEG into the chitosan film. MALDI ToF MS analysis of the degradation products was performed using various different matrices (DHB, α-CHCA and DCTB) (Fig. 4b–d).

When DHB was employed as the matrix a broad and complex distribution of species was detected (Fig. 4b). Analysis of the spectrum in the 750–1250 *m*/*z* region revealed two major series of peaks corresponding to glucosamine- and cystamine-bound PEG-based species with either 1 or 2 glucosamine repeat units. The presence of chitosan oligomers was also detected towards higher molecular weights with a series of peaks separated by 161.1 Da, which corresponds to the glucosamine repeat unit. Alternatively, when α-CHCA was used as the matrix, three major doubly charged series were observed (Fig. 4c). Between 830 and 1100 *m*/*z* these series corresponded to (i) glucosamine-capped PEG linked by cystamine, (ii) glucosamine-capped PEG groups and (iii) branched glucosamine capped with three PEG groups and linked by cystamine. Using DCTB as the matrix provided a spectrum with two major series corresponding to PEG-functionalized glucosamine series and glucosamine-capped PEG series (Fig. 4d). In addition to the series presented in Fig. 4b–d, other multibranched PEG series bound with cystamine and glucosamine (results not shown) were also observed. The complementary results obtained from MALDI ToF MS and ^{1}H NMR spectroscopic analysis provide good evidence for the structure of the degradation products and indicate that the CPHFs are comprised of chitosan chains cross-linked with PEG and PEG/cystamine combinations.

3.5. Mechanical evaluation of CPHFs

To investigate the effect of PEG cross-linking on the films' mechanical properties, tensile testing was performed to determine the ultimate stress (σ), fracture strain (ultimate elongation, %ε) and elastic moduli (E) of the unmodified and cross-linked chitosan

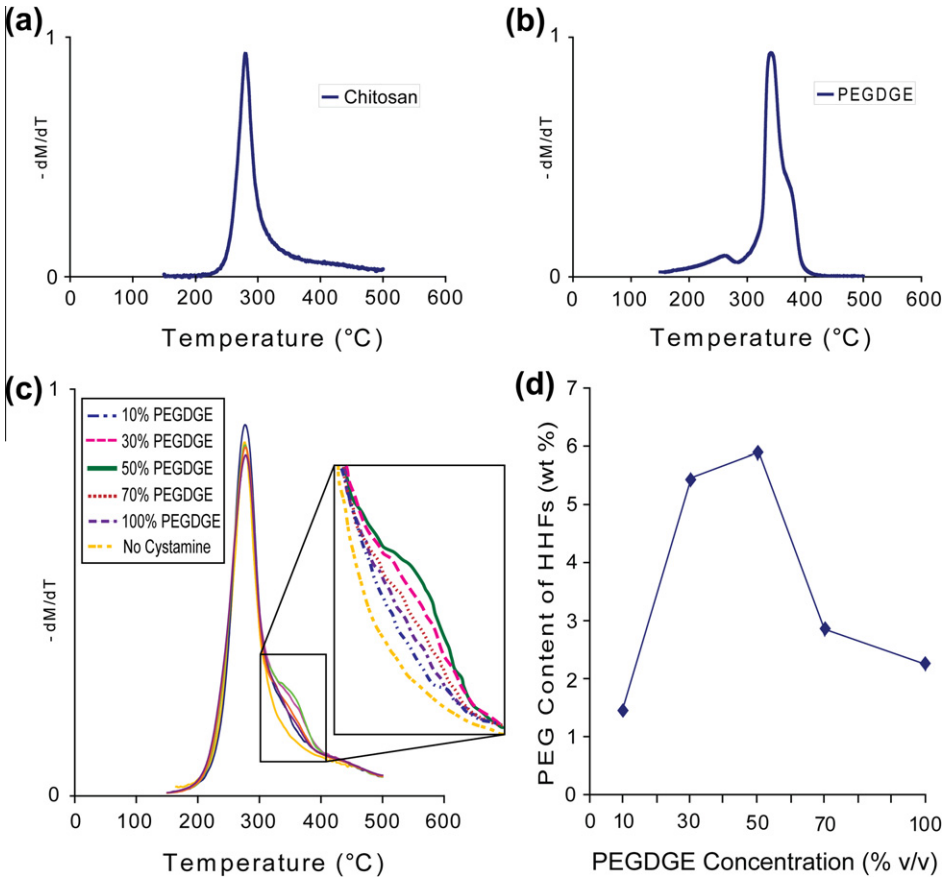

Fig. 3. First-derivative thermogravimetric curves for (a) chitosan film, (b) PEGDGE and (c) CPHFs cross-linked using various concentrations of PEGDGE with and without cystamine. (d) PEG content of CPHFs.

Table 1
Water content of unmodified chitosan film and CPHFs.

Material	Chitosan film	$CPHF_{10}$	$CPHF_{30}$	$CPHF_{50}$	$CPHF_{70}$	$CPHF_{100}$
%ESR	172.5 ± 9	171.4 ± 1	170.2 ± 8	171.8 ± 9	170.2 ± 5	170.3 ± 8

films (Fig. 5 and Table 2). In general, cross-linking with PEGDGE and cystamine was found to significantly enhance the σ and $\%\varepsilon$ of the chitosan film without significantly effecting the E. For example, the σ and $\%\varepsilon$ of the unmodified chitosan film were 9.9 MPa and 65%, respectively, whereas $CPHF_{50}$ had an σ and $\%\varepsilon$ of 28.2 MPa and 101%, respectively. Interestingly, the σ and $\%\varepsilon$ of the CPHFs were observed to increase and then decrease with increasing PEGDGE concentration (Fig. 5a and b), which correlates well with the wt.% of PEG determined from TGA (Fig. 3d and Table 2). The Gaussian-like trend in the PEG content of the CPHFs observed from the TGA (Fig. 3) is also replicated in the σ and $\%\varepsilon$ of the films (Fig. 5). In regards to the ultimate stresses and strains obtained from the tensile evaluation, this increase and decrease in the σ and $\%\varepsilon$ of the films correlates directly with the PEG content of CPHFs. This indicates that the σ and $\%\varepsilon$ of the films is directly related to the PEG content of the CPHFs, and most likely an increase in cross-linking density with higher PEG content. Thus, as the PEG content decreases, the improvement in σ and $\%\varepsilon$ also diminishes. The E of the CPHFs is comparable to the human cornea, which is important for modulating cell behaviour [72–74]. In comparison, the chitosan films that were treated without cystamine showed negligible difference to the unmodified chitosan films. Since no cross-linking of films treated without cystamine was observed in the TGA, the tensile properties of these films remained unchanged as expected (Fig. 5). CPHFs are designed as platforms to support attachment and proliferation of CECs. This proliferation period can take a few days or even weeks. This period, in which the CPHFs are maintained in media at 37 °C, could lead to degradation of their tensile properties. Hence CPHFs maintained in the same in vitro conditions for 14 days were subjected to tensile evaluation. From these results a small reduction in the σ and the $\%\varepsilon$ was observed (~25.4 MPa and ~95%, respectively). Compared to the human cornea, CPHFs maintain a very high σ and $\%\varepsilon$ even after 14 days in media, and hence still demonstrate suitable tensile properties for implantation following in vitro CEC proliferation. The high tensile strength and elasticity of the CPHFs make them suitable for utilization in implantation techniques such as DSEK, where a robust substrate is required to survive the physical manipulations of the surgical procedure. As a result of its high σ and $\%\varepsilon$, and comparable E to the human cornea, $CPHF_{50}$ was selected for further studies and evaluation.

3.6. In vitro permeability evaluation of CPHFs

Since the cornea receives nutrients via diffusion it is extremely important that substrates targeted towards ophthalmic applications are permeable to nutrients and other biomolecules (e.g. glucose and albumin) [75]. Therefore, the permeability of $CPHF_{50}$ to glucose and

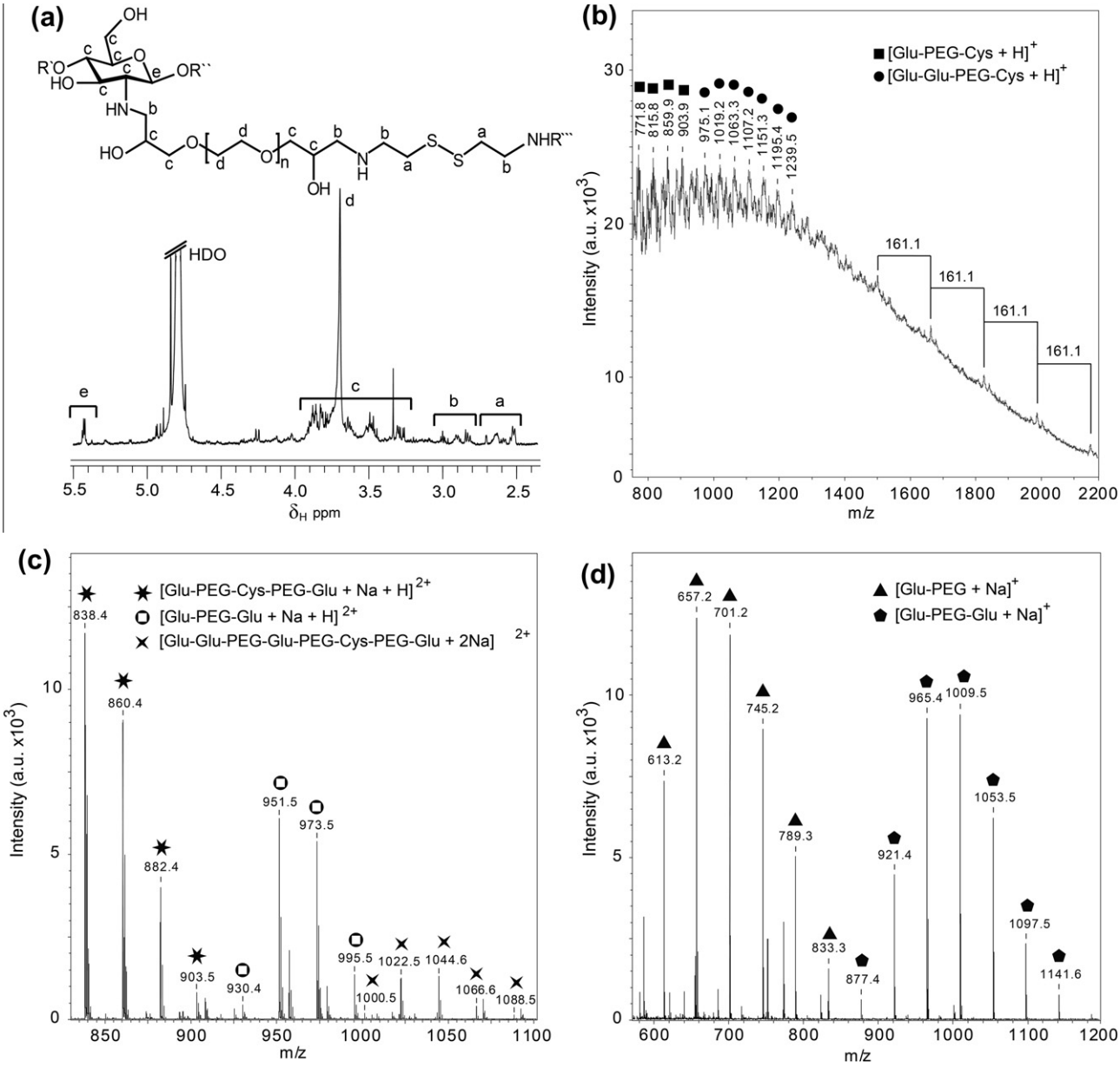

Fig. 4. (a) ^{1}H NMR spectrum (D_2O) of the residue isolated from isopropanol extraction of the CPHF degradation products. MALDI ToF mass spectra of CPHF acid degradation products recorded in linear/positive using (b) DHB, (c) α-CHCA and (d) DCTB as the matrices.

albumin was investigated in vitro using a thermostated side-by-side cell, and the diffusivity for glucose and albumin were determined to be $\sim 1.0 \times 10^{-6}$ and $\sim 1.0 \times 10^{-8}$ cm^2 s^{-1}, respectively. The human cornea has diffusivities for glucose and albumin of $\sim 2.6 \times 10^{-6}$ and $\sim 1.0 \times 10^{-7}$ cm^2 s^{-1}, respectively [31]. Thus, the glucose permeability of the CPHF is comparable to the human cornea, and even though the albumin permeability is a magnitude lower, this may still be sufficient. Further in vivo studies may demonstrate whether the diffusivity of the CPHFs is suitable for implantation. Ultimately, the in vitro permeability studies demonstrate that the CPHFs are permeable to both large and small molecules that are important for the survival and function of CECs.

3.7. In vitro degradation of CPHFs

Ideally, tissue engineering scaffolds need to degrade in a controlled manner and allow the restoration of the target tissue to its natural structure, morphology and function without leaving any foreign material behind. Chitosan is readily degraded by enzymes via the cleavage of the glycosidic bonds, specifically lysozyme, which is naturally present in various parts of the human body and notably in tears [76,77]. To assess the degradability of the films, $CPHF_{50}$ was subjected to an accelerated in vitro degradation study using lysozyme and L-cysteine. $CPHF_{50}$ was selected as an example to demonstrate the degradation capacity of a cross-linked CPHF. The naturally occurring L-cysteine was included in the degradation solution to aid in the cleavage of the disulfide bonds present in the cross-links as a result of the inclusion of cystamine during the cross-linking process. Degradation of $CPHF_{50}$ using lysozyme and L-cysteine at concentrations of 100 times greater than those in the human aqueous humour resulted in a mass loss of ~50% after 55 days (Fig. 6). Evidently, slower degradation would be expected in vivo as a result of lower concentrations of lysozyme and L-cysteine, although the presence of other enzymes or bioactive molecules (e.g. glutathione) could play a role in degradation of the films. For example, chitosan degradation by

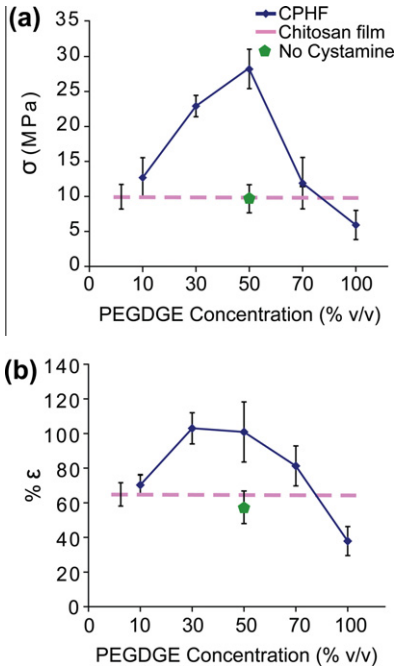

Fig. 5. Comparisons of the effects of PEGDGE concentration during cross-linking on CPHFs: (a) ultimate stresses (σ); (b) ultimate strains ($\%\varepsilon$).

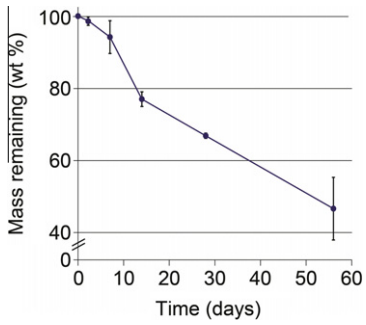

Fig. 6. In vitro degradation profile of $CPHF_{50}$ over a 55 day time period.

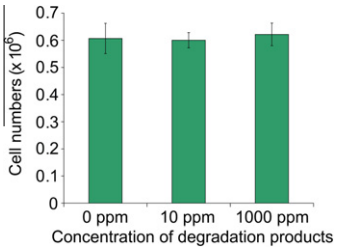

Fig. 7. Comparison of 3T3 proliferation after 72 h in the absence (control, 0 ppm), and presence of 10 and 1000 ppm of CPHF degradation products.

non-specific enzymes present in the human body (e.g. collagenase) has been reported [78–80]. Regardless, a slower degradation rate may be more favourable to allow the cell's natural migration to maintain a confluent corneal endothelium and migrate to the corneal stromal surface as the film is degraded and cleared from the anterior chamber of the cornea. Furthermore, follow-up inspections for the DSEK procedures can range from 6 to 18 months, which is within the degradation time frame of the CPHFs [11,65,8]. Other studies have shown that the degradation rate of PEG-blended/modified chitosan films can vary depending on the PEG content as well as cross-linking density [81–83]. Since the PEG content of the CPHFs can be tailored via the variation of the PEGDGE concentration during cross-linking, this may allow control of the degradation rate of the CPHFs. Nevertheless, this study demonstrates that the CPHFs are biodegradable in the presence of lysozyme and L-cysteine, which are naturally present in the cornea.

3.8. Cytotoxicity assessment of CPHF degradation products

As CPHFs are potential implantation materials, it is crucial that their degradation products are benign and demonstrate negligible toxicity. Therefore, $CPHF_{50}$ was completely degraded under acidic conditions in an accelerated manner and the degradation products were isolated, analyzed and subjected to in vitro cytotoxicity studies with 3T3 fibroblasts. Initially, $CPHF_{50}$ was degraded using concentrated HCl and the excess HCl was completely removed to afford a light brown powder. The cytotoxicity of the degradation products was evaluated via a standard cell proliferation study, whereby 3T3 cell suspensions of known cell number were incubated in the presence of 10 and 1000 ppm of the degradation products for a period of 72 h. For both concentrations studied the cells proliferated at the same rate as that of the control (Fig. 7), implying that the acid-catalyzed degradation products do not impair cell growth and are benign. It is likely that the degradation products that would result from degradation by lysozyme in vivo are large chitosan oligomers and cross-linked PEG chains. HCl degradation degrades chitosan to much shorter glucosamine oligomers covalently attached to PEG as observed in the NMR and MALDI ToF studies. Even though they are not identical to the in vivo degradation products in regards to their molecular weight, by composition they are similar. Ultimately, in vivo cytotoxicity studies would need to be conducted to confirm the toxicity of the CPHFs, but these studies are outside the scope of this manuscript.

Table 2
Mechanical properties of unmodified chitosan films, PEGDGE-modified films without cystamine, CPHFs, and human cornea.

Material[a]	PEG content wt.%[b]	Ultimate stress (σ)/MPa[c]	Fracture strain ($\%\varepsilon$)[c]	Tensile modulus (E)/MPa[c]
Chitosan film	–	9.9 ± 1.6	65 ± 12	15.5 ± 2.7
No cystamine film	–	9.8 ± 1.8	56 ± 15	17.6 ± 4.3
$CPHF_{10}$	1.5	12.7 ± 2.9	70 ± 6	12.5 ± 1.8
$CPHF_{30}$	5.4	22.9 ± 1.5	103 ± 9	14.3 ± 5.1
$CPHF_{50}$	5.9	28.2 ± 3.3	101 ± 17	17.7 ± 6.6
$CPHF_{70}$	2.8	11.9 ± 3.7	81 ± 12	12.6 ± 0.8
$CPHF_{100}$	2.3	5.9 ± 2.1	38 ± 8	10.4 ± 3.4
Human cornea[d]	–	3.3 ± 0.2	60 ± 15	15.9 ± 2.0

[a] CPHF refers to chitosan–PEG hydrogel film and the subscript number refers to the concentration (% v/v) of PEGDGE used in the cross-linking solution.
[b] Determined by TGA.
[c] Determined via tensile mechanical testing.
[d] Values taken from Ref. [31].

3.9. In vitro CEC attachment and proliferation on CPHFs

Ultimately, the CPHFs need to be able to support the attachment, migration and proliferation of CECs if they are to be used as substrates for CEC regeneration and transplantation. In this study, preliminary in vitro CEC culture experiments were conducted using primary cells of sheep origin, demonstrating that the CPHFs have the capacity to support the attachment and proliferation of CECs. CECs were isolated by first carefully microdissecting the Descemet's membrane. This membrane is a thick ECM which is covered by a monolayer of pure CECs. This isolation technique purifies CECs, removing other cell types. The cells are removed from the Descemet's membrane by digestions first with collagenase, and then trypsinized before being resuspended in corneal media. The cultured CECs retained their natural in vivo polygonal morphology (Fig. 8a and b). CAST counting of cells cultured on CPHF gave a cell density of 4499 cell mm^{-2} ($n = 2$, 4071, 4926). CAST determined the CPHF area to be 111.7 mm^2; this indicates a total cell number of ~470 000 cells after 7 days, which is a 9-fold increase in cell number from the 50 000 cells seeded initially. A film seeded with 25 000 cells achieved a cell density of 3747 cell mm^{-2}. These cell densities are slightly higher than that of sheep CEC in vivo, which were determined to be 3150 (SE = 88, $n = 3$) by specular microscopy, and 3428 cell mm^{-2} ($n = 2$, 2433, 4423) by CAST. This is because it was observed at 7 days of culture that the cells were slightly overgrown. Immunofluorescence demonstrates that cultured cells are positive to Na^+/K^+-ATPase (Fig. 8c and d). Na^+/K^+-ATPase is a regulator of pump function [84,85]. Na^+/K^+-ATPase has been used previously as a marker for CECs [86,87]. The presence of Na^+/K^+-ATPase at the lateral periphery is indicative of intact pump function [85]. Although sheep CECs are delicate cells that naturally do not have a replicative capability in vivo [3,88], they were able to readily proliferate on the CPHFs. The in vitro capability of the CPHFs to support the attachment, migration and proliferation of CECs indicates their potential application to corneal tissue engineering.

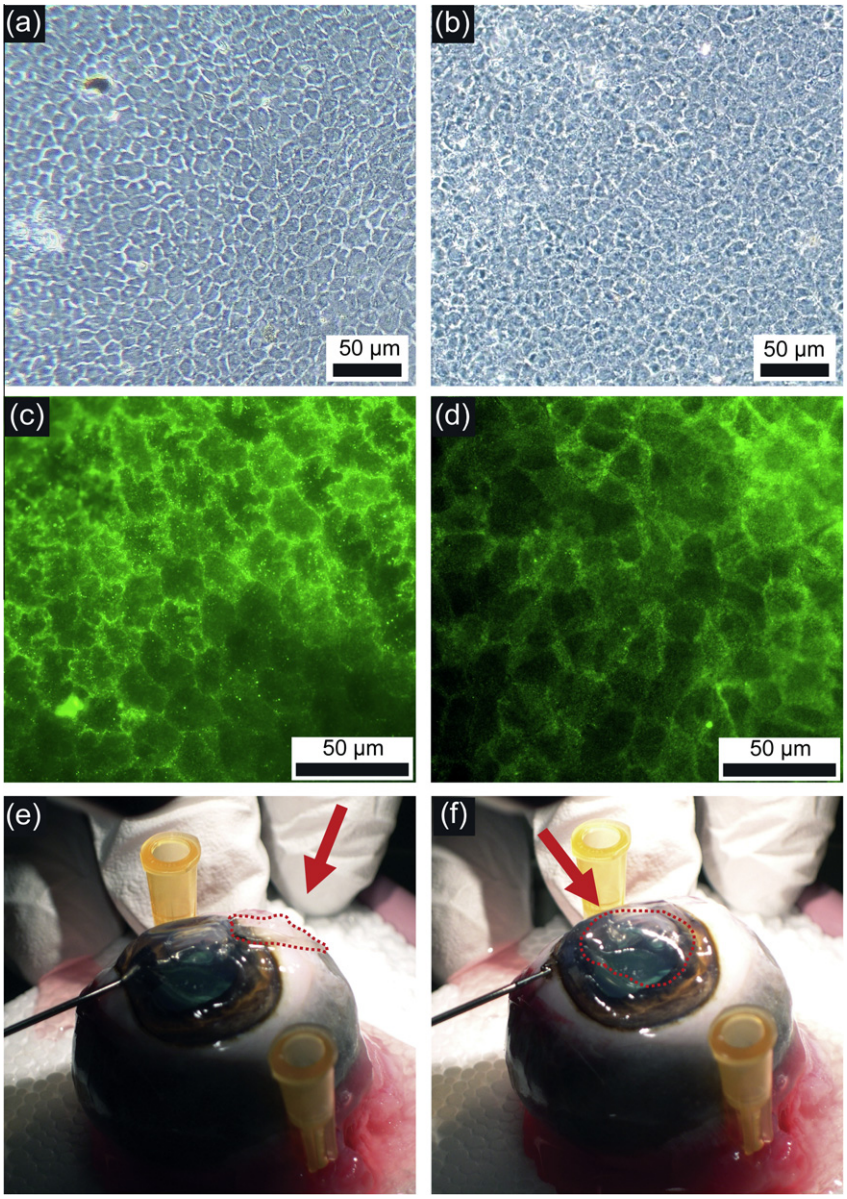

Fig. 8. Comparison of ovine CECs cultured on (a) TCP and (b) CPHF surface (7 days). Na^+/K^+-ATPase immunostaining on (c) CECs on native sheep Descemet's membrane, (d) CECs on CPHF (gamma adjusted to minimize background autofluorescence from CPHF). Ex vivo evaluation of CPHF implantation (e) before and (f) after insertion into the ovine anterior chamber.

3.10. Ex vivo surgical evaluation of CPHFs using ovine eyes

Ex vivo evaluation was carried out using ovine eyes to determine the applicability of the CPHFs in the DSEK surgical procedure. Small incisions were made on opposite sides of the ovine cornea and the CPHF was pulled into the anterior chamber using fine vitreo-retinal forceps. The excellent mechanical properties allowed facile manipulation of the CPHF during the procedure and it was easily pulled into the anterior chamber of the ovine eye (Fig. 8e and f). The insertion of the film did not require any instrumental aids such as a Busin's glide or sutures [89,90], and following insertion the films remained flat and unfolded, and easily adhered onto the interior corneal surface with minimal physical assistance. The ex vivo surgical evaluation demonstrates that the CPHFs are excellent platforms for transplantation of CECs via a DSEK-like procedure as a result of their robustness and ease of handling.

4. Conclusions

Ultrathin CPHFs were successfully fabricated using a new method of post-cross-linking via epoxy–amine chemistry. The CPHFs were found to possess excellent mechanical properties. The tensile modulus of the CPHFs was engineered to be comparable with that of the cornea to provide a favourable mechanoresponsive environment for CECs. The robust mechanical properties and hydrated film thickness of just 50 μm make the CPHFs excellent candidates for minimally invasive surgical procedures, such as DSEK, as demonstrated by ex vivo surgery with ovine eyes. The transmission of visible light through the CPHFs was found to be greater than 95% and they were readily permeable to glucose and albumin, which makes them highly suitable for ophthalmic applications. In vitro degradation of the CPHFs in the presence of lysozyme and L-cysteine over an 8 week period demonstrated that the CPHFs are biodegradable and in vitro cell proliferation studies revealed that the acid-catalyzed degradation products are benign. Naturally non-proliferative CECs from sheeps were successfully grown to confluence on the CPHFs. Thus, the CPHFs demonstrate excellent mechanical, optical, permeable and biocompatible properties that make them desirable candidates as substrates for the attachment, proliferation and implantation of CECs.

Acknowledgements

We thank the Ophthalmic Research Institute of Australia (ORIA) for funding, Dr Andrea O'Connor (Department of Chemical and Biomolecular Engineering, The University of Melbourne) for use of facilities, Katrina Harris for experimental assistance, and Filmetrics for spectral reflectance measurements. Corneal confocal microscopy was carried out by Adrienne Mackey from Lions Eye Donation Service, Centre for Eye Research Australia (CERA). The MALDI ToF MS used in these studies was supported under Australian Research Council's Linkage Infrastructure, Equipment and Facilities (LIEF) funding scheme (LE0882576).

Appendix A. Figures with essential color discrimination

Certain figures in this article, particularly Figs. 1–3 and 5–8, are difficult to interpret in black and white. The full color images can be found in the on-line version, at http://dx.doi.org/10.1016/j.actbio.2013.01.020.

References

[1] Engelmann K, Bednarz J, Valtnik M. Prospects for endothelial transplantation. Exp Eye Res 2004;78:573–8.
[2] Peh GSL, Beuerman RW, Colman A, Tan DT, Mehta JS. Human corneal endothelial cell expansion for corneal endothelium transplantation: an overview. Transplantation 2011;91(8):811–9.
[3] Joyce NC. Proliferative capacity of the corneal endothelium. Prog Retin Eye Res 2003;22:359–89.
[4] Armitage WJ, Tullo AB, Larkin DFP. The first successful full-thickness corneal transplant: a commentary on Eduard Zirm's landmark paper of 1906. Br J Ophthalmol 2006;90:1222–3.
[5] Melles GRJ, Eggink F, Lander F, Pels E, Rietveld FJR, Beekhuis WH, et al. A surgical technique for posterior lamellar keratoplasty. Cornea 1998;17(6):618–26.
[6] Melles GRJ, Ong TS, Ververs B, van der Wees J. Descemet membrane endothelial keratoplasty. Cornea 2006;25(8):987–90.
[7] Dapena I, Ham L, Melles GRJ. Endothelial keratoplasty: DSEK/DSAEK or DMEK – the thinner the better? Curr Opin Ophthalmol 2009;20:299–307.
[8] Price FW, Price MO. Descemet's stripping with endothelial keratoplasty in 50 eyes: a refractive neutral corneal transplant. J Refract Surg 2005;21(4):339–45.
[9] Kwon RO, Price MO, Price FW, Ambrósio R, Belin MW. Pentacam characterization of corneas with Fuchs dystrophy treated with Descemet membrane endothelial keratoplasty. J Refract Surg 2010;26(12):972–9.
[10] Jordan CS, Price MO, Trespalacios R, Price FW. Graft rejection episodes after Descemet stripping with endothelial keratoplasty: part one: clinical signs and symptoms. Br J Ophthalmol 2009;93(3):387–90.
[11] Mearza AA, Qureshi MA, Rostron CK. Experience and 12-month results of Descemet-stripping endothelial keratoplasty (DSEK) with a small-incision technique. Cornea 2007;26:279–83.
[12] Liu W, Merret K, Griffith M, Fagerholm P, Dravida S, Heyne B, et al. Recombinant human collagen for tissue engineered corneal substrates. Biomaterials 2008;29:1147–58.
[13] Crabb RAB, Chau EP, Evans MC, Barocas VH, Hubel A. Biomechanical and microstructural characteristics of a collagen film-based corneal stroma equivalent. Tissue Eng 2006;12(6):1565–75.
[14] Merret K, Fagerholm P, McLaughlin CR, Dravida S, Lagali N, Shinozaki N, et al. Tissue-engineered recombinant human collagen-based corneal substitutes for implantation: performance of Type I versus Type III collagen. Invest Ophthalmol Vis 2008;49(9):3887–94.
[15] Mimura T, Yamagami S, Yokoo S, Usui T, Tanaka K, Hattori S, et al. Cultured human corneal endothelial cell transplantation with a collagen sheet in a rabbit model. Invest Ophthalmol Vis 2004;45(9):2992–7.
[16] Mohay J, Lange TM, Soltau JB, Wood TO, McLaughlin BJ. Transplantation of corneal endothelial cells using a cell carrier device. Cornea 1994;13(2):173–82.
[17] Hadlock T, Singh S, Vacanti JP, McLaughlin BJ. Ocular cell monolayers cultured on biodegradable substrates. Tissue Eng 1999;5(3):187–96.
[18] Engelman K, Drexler D, Böhnke M. Transplantation of adult human or porcine corneal endothelial cells onto human recipients in vitro. Part I: Cell culturing and transplantation procedure. Cornea 1999;18(2):199–206.
[19] Böhnke M, Eggli P, Engelmann K. Transplantation of adult human or porcine corneal endothelial cells onto human recipients in vitro. Part II: Evaluation in the scanning electron microscope. Cornea 1999;18(2):207–13.
[20] Liang Y, Liu W, Han B, Yang C, Ma Q, Zhao W, et al. Fabrication and characters of a corneal endothelial cells scaffold based on chitosan. J Mater Sci Mater Med 2011;22:175–83.
[21] Kim S, Healy KE. Synthesis and characterisation of injectable poly(N-isopropylacrylamide-co-acyrlic acid) hydrogels with proteolytically degradable cross-links. Biomacromolecules 2003;4:1214–23.
[22] Adds PJ, Hunt CJ, Dart JKG. Amniotic membrane grafts, "fresh" or "frozen? A clinical and in vitro comparison. Br J Ophthalmol 2001;85:905–7.
[23] Lu PL, Lai JY, Ma DHK, Hsiue GH. Carbodiimide cross-linked hyaluronic acid hydrogels as cell sheet delivery vehicles: characterisation and interaction with corneal endothelial cells. J Biomater Sci Polymer Edn 2008;19(1):1–18.
[24] Ishino Y, Sano Y, Nakamura T, Connon CJ, Rigby H, Fullwood NJ, et al. Amniotic membrane as a carrier for cultivated human corneal endothelial cell transplantation. Invest Ophthalmol Vis Sci 2004;45(3):800–6.
[25] Madden PW, Lai JNX, George KA, Giovenco T, Harkin DG, Chirila TV. Human corneal endothelial cell growth on silk fibroin membrane. Biomaterials 2011;32:4076–84.
[26] Kadajji VG, Betager GV. Water soluble polymers for pharmaceutical applications. Polymers 2011;3:1972–2009.
[27] Cao Y, Wang B. Biodegradation of silk biomaterials. Int J Mol Sci 2009;10:1514–24.
[28] Sell SA, Wolfe PS, Garg K, McCool JM, Rodriguez IA, Bowlin GL. The use of natural polymers in tissue engineering: a focus on electrospun extracellular matrix analogues. Polymers 2010;2:522–53.
[29] Saw VPJ, Minassian D, Dart JKG, Ramsay A, Henderson H, Poniatowski S, et al. Amniotic Membrane Tissue User Group. Amniotic membrane transplantation for ocular disease: a review of the first 233 cases from the UK user group. Br J Ophthalmol 2007;91:1042–7.
[30] Connon CJ, Doutch J, Chen B, Hopkinson A, Mehta JS, Nakamura T, et al. The variation in the transparency of amniotic membrane used in ocular surface regeneration. Br J Ophthalmol 2010;94:1057–61.
[31] Rafat M, Li F, Fagerholm P, Lagali NS, Watsky MA, Munger R, et al. PEG-stabilised carbodiimide crosslinked collagen–chitosan hydrogels for corneal tissue engineering. Biomaterials 2008;29:3960–72.
[32] Zhang H, Neau SH. *In vitro* degradation of chitosan by a commercial enzyme preparation: effect of molecular weight and degree of deacetylation. Biomaterials 2001;22:1653–8.

[33] Bhattarai N, Ramay HR, Gunn J, Matsen FA, Zhang M. PEG-grafted chitosan as an injectable thermosensitive hydrogel for sustained protein release. J Control Release 2005;103:609–24.
[34] Beibuth S, Chanachai A, Jiraratananon. Modification of PVDF membrane by chitosan solution for reducing protein fouling. J Membrane Sci 2009;342:97–104.
[35] Rabea EI, Badawy MET, Stevens CV, Smagghe G, Steurbaut W. Chitosan as antimicrobial agent: applications and mode of action. Biomacromolecules 2003;4(6):1457–65.
[36] Pilai CKS, Paul W, Sharma CP. Chitin and chitosan polymers: chemistry, solubility and fiber formation. Prog Polym Sci 2009;34:641–78.
[37] Muzzarelli RAA. Chitins and chitosans for the repair of wounded skin, nerve, cartilage and bone. Carbohydr Polym 2009;76:167–82.
[38] Shi C, Zhu Y, Ran X, Wang M, Su Y, Cheng T. Therapeutic potential of chitosan and its derivatives in regenerative medicine. J Surg Res 2006;133:185–92.
[39] Jiang T, Kumbar SG, Nair LS, Laurencin CT. Biologically active chitosan systems for tissue engineering and regenerative medicine. Curr Top Med Chem 2008;8:354–64.
[40] Muzzarelli RAA. Genipin crosslinked chitosan hydrogels as biomedical and pharmaceutical aids. Carbohydr Polym 2009;77:1–9.
[41] Jin R, Teixeira LSM, Dijkstra PJ, Karperien M, van Blitterswijk CA, Zhong ZY, et al. Injectable chitosan-based hydrogels for cartilage tissue engineering. Biomaterials 2009;30(13):2544–51.
[42] Tan HP, Rubin JP, Marra KG. Injectable in situ forming biodegradable chitosan-hyaluronic acid based hydrogels for adipose tissue regeneration. Organogenesis 2010;6(3):173–80.
[43] Boucard N, Viton C, Agay D, Mari E, Roger T, Chancerelle Y, et al. The use of physical hydrogels of chitosan for skin regeneration following third degree burns. Biomaterials 2007;28(24):3478–88.
[44] Ronda L, Bruno S, Abbruzzetti S, Viappiani C, Bettati S. Ligand reactivity and allosteric regulation of haemoglobin based oxygen carriers. Biochim Biophys Acta 2008;1784:1365–77.
[45] Bailon P, Berhtold W. Polyethylene glycol-conjugated pharmaceutical proteins. Pharm Sci Technol Today 1998;1(8):352–6.
[46] Kim DN, Lee W, Koh WG. Preparation of protein microarrays on non-fouling and hydrated poly(ethylene glycol) hydrogel substrates using photochemical surface modification. J Chem Technol Biotechnol 2009;84:279–84.
[47] Quirk RA, Davies MC, Tendler SJB, Chan WC, Shakesheff KM. Controlling biological interactions with poly(lactic acid) by surface entrapment modification. Langmuir 2001;17:2817–20.
[48] Tan H, DeFail AJ, Rubin JP, Chu CR, Marra KG. Novel multiarm PEG-based hydrogels for tissue engineering. J Biomed Res A 2010;92A(3):979–87.
[49] Han DK, Park KD, Hubbel JA, Kim YH. Surface characteristics and biocompatibility of lactide-based poly(ethylene glycol) scaffolds for tissue engineering. J Biomat Sci Polym E 1998;9(7):667–80.
[50] Park JS, Woo DG, Sun BK, Chung HM, Im SJ, Choi Ym, et al. *In vitro* and *in vivo* test of PEG/PCL-based hydrogel scaffold for cell delivery application. J Control Release 2007;124(1–2):51–9.
[51] Park CH, Hong YJ, Park K, Han DK. Peptide-grafted lactide-based poly(ethylene glycol) porous scaffolds for specific cell adhesion. Macromol Res 2010;18(5):526–32.
[52] Hamid ZAA, Blencowe A, Ozcelik B, Palmer JA, Stevens GW, Abberton KM, et al. Epoxy-amine synthesised hydrogel scaffolds for soft-tissue engineering. Biomaterials 2010;31:6454–67.
[53] Hong H, Liu C, Wu W. Preparation and characterisation of PEG/chitosan/gelatin composites for tissue engineering. J Appl Polym Sci 2009;114:1220–5.
[54] Li F, Ba Q, Niu S, Gup Y, Duan Y, Zhao P, et al. In-site forming biodegradable glycol chitosan-based hydrogels: synthesis, characterisation and chondrocyte culture. Mater Sci Eng C 2012;32:2017–25.
[55] Wang JW, Hon MH. Sugar-mediated chitosan/poly(ethylene glycol)-β-dicalcium pyrophosphate composite: mechanical and microstructural properties. J Biomed Mater Res A 2003;64A(2):262–72.
[56] Yang J, Klassen H, Pries M, Wang W, Nissen MH. Aqueous humor enhances the proliferation of rat retinal precurson cells in culture and this effect is partially reproduced by ascorbic acid. Stem Cells 2006;24(12):2766–75.
[57] Richer ST, Rose RC. Water soluble antioxidants in mammalian aqueous humor: interaction with UV B and hydrogen peroxide. Vision Res 1998;38:2881–8.
[58] Duchet J, Pascault JP. Do epoxy-amine networks become inhomogenous at the nanometric scale? J Polym Sci Pol Chem 2003;41:2422–32.
[59] Zvetkov VL. A modified kinetic model of poxy-amine reaction. Macromol Chem Phys 2002;203:467–76.
[60] Tahami SHV, Ranjbar Z, Bastani S. Preparation and stability behaviour of the colloidal epoxy-1,1-iminodi-2-propanol adducts. Prog Org Coat 2011;71(3):234–41.
[61] Bonnet A, Pascault JP, Sautereau H, Taha M, Camberlin Y. Epoxy-diamine thermoset/thermoplastic blends. 1. Rates of reactions before and after phase separation. Macromolecules 1999;32:8517–23.
[62] Peesan M, Sirivat A, Supaphol P, Rujiravanit R. Dilute solution properties of hexanoyl chitosan in chloroform, dichloromethane and tetrahydrofuran. Carbohydr Polym 2006;64:175–83.
[63] Ahmed KA, McLaren JW, Baratz KH, Maguire LJ, Kittleson KM, Patel SV. Host and graft thickness after Descemet stripping endothelial keratoplasty for Fuchs endothelial dystrophy. Am J Ophthalmol 2010;150:490–7.
[64] Tarnawska D, Wylegala E. Monitoring cornea and graft morphometric dynamics after Descemet stripping and endothelial keratoplasty with anterior segment optical coherence tomography. Cornea 2010;29:272–7.
[65] Lu PL, Lai JY, Ma DHK, Hsiue GH. Carbodiimide cross-linked hyaluronic acid hydrogels as cell sheet delivery vehicles: characterization and interaction with corneal endothelial cells. J Biomater Sci Polym E 2008;19(1):1–18.
[66] Lai JY, Lu PL, Chen KH, Tabata Y, Hsiue GH. Effect of charge and molecular weight on the functionality of gelatin carriers for cornea endothelial cell therapy. Biomacromolecules 2006;7:1836–44.
[67] Doutch JJ, Quantock AJ, Joyce NC, Meek KM. Ultraviolet light transmission through the human corneal stroma is reduced in the periphery. Biophys J 2012;102:1258–64.
[68] Doutch JJ, Quantock AJ, Smith VA, Meek KM. Light transmission in the human cornea as a function of position across the ocular surface. theoretical and experimental aspects. Biophys J 2008;95:5092–9.
[69] Beems EM, Best JAV. Light transmission of the cornea in whole human eyes. Exp Eye Res 1990;50:393–5.
[70] Trombotto S, Ladaviere C, Delolme F, Domard A. Chemical preparation and structural characterization of a homogenous series of chitin/chitosan oligomers. Biomacromolecules 2008;9:1731–8.
[71] Yan X, Evenocheck HM. Chitosan analysis using acid hydrolysis and HPLC/UV. Carbohydr Polym 2012;87(2):1774–8.
[72] Pelham RJ, Wang YL. Cell locomotion and focal adhesions are regulated by substrate flexibility. Proc Natl Acad Sci USA 1997;94:13661–5.
[73] Byfield FJ, Levental I, Nordstrom K, Arratia PE, Miller RT, Janmey PA. Absence of Filamin A prevents cells from responding to stiffness gradients on gels coated with collagen but not fibronectin. Biophys J 2009;96:5095–102.
[74] Reinhart-King CA, Dembo M, Hammer DA. Cell-cell mechanical communication through compliant substrates. Biophys J 2008;95:6044–51.
[75] Liu L, Sheardown H. Glucose permeable poly(dimethyl siloxane) poly (N-ispropyl acrylamide) interpenetrating networks as ophthalmic biomaterials. Biomaterials 2005;26:233–44.
[76] Ren D, Yi H, Wang W, Ma X. The enzymatic degradation and swelling properties of chitosan matrices with different degrees of N-acetylation. Carbohydr Res 2005;340:2403–10.
[77] Yang YM, Hu W, Wang XD, Gu XS. The controlling biodegradation of chitosan fibers by N-acetylation *in vitro* and *in vivo*. J Mater Sci Mater Med 2007;18:2117–21.
[78] Lim SM, Song DK, Oh SH, Yoon DSL, Bae EH, Lee JH. *In vitro* and *in vivo* degradation behaviour of acetylated chitosan porous beads. J Biomat Sci Polym E 2008;19(4):453–66.
[79] Kulish EI, Volodina VP, Kolesov SV, Zaikov GE. Enzymatic degradation of chitosan films by collagenase. Polym Sci Ser B 2006;48(9–10):244–6.
[80] Kulish EI, Volodina VP, Fatkullina RR, Kolesov SV, Zaikov GE. Enzymatic degradation of chitosan films under the action of nonspecific enzymes. Polym Sci Ser B 2008;50(7–8):175–6.
[81] Tanuma H, Kiuchi H, Kai W, Yazawa K, Inoue Y. Characterization and enzymatic degradation of PEG-cross-linked chitosan hydrogel films. J Appl Polym Sci 2009;114:1902–7.
[82] Tanuma H, Saito T, Nishikawa K, Dong T, Yazawa K, Inoue Y. Preparation and characterization of PEG-cross-linked chitosan hydrogel films with controllable swelling and enzymatic degradation behaviour. Carbohydr Polym 2010;80:260–5.
[83] Altinisik A, Yurdakoc K. Synthesis, characterization, and enzymatic degradation of chitosan/PEG hydroel films. J Appl Polym Sci 2011;122:1556–63.
[84] Riley MV. Anion-sensitive ATPase in rabbit corneal endothelium and its relation to corneal hydration. Exp Eye Res 1977;25:483–94.
[85] McCartney MD, Robertson DP, Wood TO, McLaughlin BJ. ATPase pump site density in human dysfunctional corneal endothelium. Invest Ophthalmol Vis Sci 1987;28:1955–62.
[86] Lai JY, Chen KH, Hsu WM, Hsiue GH, Lee YH. Bioengineered human corneal endothelium for transplantation. Arch Ophthalmol 2006;124:1441–8.
[87] Sumide T, Nishida K, Yamato M, Ide T, Hayashida Y, Watanabe K, et al. Functional human corneal endothelial cell sheets harvested from temperature-responsive culture surfaces. FASEB J 2006;20:392–4.
[88] Klebe S, Sykes PJ, Coster DJ, Krishnan R, Williams KA. Prologation of sheep corneal allograft survival by ex vivo transfer of the gene encoding interleukin-10. Transplantation 2001;71(9):1214–20.
[89] Macsai MS, Kara-Jose AC. Suture technique for Descemet stripping and endothelial keratoplasty. Cornea 2007;26(9):1123–6.
[90] Bahar I, Kaiserman I, Sansanayudh W, Levinger E, Rootman DS. Busin glide vs forceps for the insertion of the donor lenticule in Descemet stripping automated endothelial keratoplasty. Am J Ophthalmol 2009;147:220–6.